Proceedings IRF2018: 6th International Conference Integrity-Reliability-Failure
Lisbon/Portugal 22-26 July 2018. Editors J.F. Silva Gomes and S.A. Meguid
Publ. INEGI/FEUP (2018); ISBN: 978-989-20-8313-1

PAPER REF: 7127

DUCTILITY OF TITANIUM ALLOYS IN A WIDE RANGE OF STRAIN RATES

Vladimir V. Skripnyak(*), Vladimir A. Skripnyak, Evgeniya G. Skripnyak
National Research Tomsk State University, Tomsk, Russia
(*)*Email:* skrp2012@yandex.ru

ABSTRACT

The aim of this work was to evaluate the combined effect of stress triaxiality and strain rate on the tensile behavior of the titanium alloy. The results of experimental studies and numerical modelling of the mechanical behavior of alpha titanium alloys were received and summarized. This paper presents the results of research on mechanical behavior of titanium alloy VT 5-1 (this is an analog of Ti-5Al-22,5Sn) in a wide range of strain rates (from 0.001 to 1000 1/s) and stress triaxiality (0.0-0.6). Specimens of four different shapes were used in experiments to study the deformation and fracture under uniaxial tension, shear. Experimental studies were performed on servo-hydraulic test machine Instron VHS 40/50-20. The model of inelastic deformation and ductile damage criterion were proposed to describe the ductility of the titanium alloy in a wide range of strain rates and stress triaxiality.

Keywords: stress triaxiality, titanium alloys, ductility, strain rates.

INTRODUCTION

There is evidence that the fracture of the hexagonal close packed polycrystalline metals and alloys is strongly dependent on the accumulated plastic strain, represented by the equivalent plastic strain, and hydrostatic pressure. The hydrostatic pressure is represented by the dimensionless stress triaxiality η ($\eta = - p/\sigma_{eq}$) defined as the ratio between the hydrostatic stress p and equivalent stress σ_{eq}. A significant distinction has been noted between the regimes of high and low stress triaxiality. The Gurson-Tvergaard-Needleman (GTN) plasticity and failure model can be complemented with phenomenological laws for void nucleation, growth and coalescence (Bai, 2008; Tvergaard, 2015).

Recently, Bobbili et al. presented modification Johnson-Cook model which provides better description on the influence of strain rate, stress triaxiality and temperature on the plastic flow of β-phase Ti-10V-2Fe-3Al alloy (Bobbili, 2016). The modified Johnson-Cook strain fracture criterion was proposed to predict the plasticity of α+β phases Ti6Al4V titanium alloy sheets deformed over a wide temperature range (295 - 1173 K) and stress states (Valoppi, 2017).

In this research we study the influence of different stress triaxiality ($0.0< \eta < 0.6$) on ductile fracture of α-phase VT 5-1 (Ti-5Al-22,5Sn) alloy in a wide range of strain rates using experimental tests and numerical simulation. Four types of VT 5-1 sheet samples were used in experiments on static and dynamic tension.

MATERIAL AND SAMPLES

The investigated material is VT 5-1 (Ti-5Al-2,5Sn) alpha phase titanium alloy. This is typically used in the aerospace field for critical aircraft components. The thickness of sheets samples was 1.15±0.05 mm. Table 1 shows that the chemical composition of VT 5-1. VT 5-1 consists of a majority of the hexagonal close packed alpha-phase. The average grain size in the sheet of VT5-1 alloy ~40 μm was determined by the method of diffraction of backscattered electrons (EBSD) (Skripnyak, 2017).

Table 1 - Chemical composition (weight percent) of VT 5-1 (Ti-5Al-22,5Sn) sheets

	Fe	**V**	**Al**	**Sn**	**Zr**	**C**	**O**	**N**	**Ti**
Composition	0.3	1.2	6.27	2.2	0.3	0.009	0.15	0.05	balance

VT 5-1 alloy is analog of Ti- 5Al-2.5Sn (Grade 6) alpha phase titanium alloy.

The tensile tests were performed on samples characterized by different geometries, as shown in Figure 1(a), in order to vary both the stress triaxiality and Lode parameter.

The stress triaxiality η and Lode parameters L defined as:

$$\eta = - p/\sigma_{eq},\ L = (2\ \sigma_{II} - \sigma_{I} - \sigma_{III})/(\sigma_{I}-\sigma_{III}), \quad (1)$$

where p is the pressure, σ_I, σ_{II}, σ_{III} are first, second, and third invariants of the Cauchy stress tensor respectively, $\sigma_{eq} = (3\ \sigma_{II})^{1/2}$ is the equivalent stress.

The stress triaxiality during the deformation is not constant. The initial triaxiality was calculated in the undeformed state by formula (Selini, 2013):

$$\eta = (1+2D)/(3\sqrt{D^2+D+1}\ ,\ D = \ln[1+a/(4R)]\,, \quad (2)$$

where: a is the width of a sample and R is the value of notch radius.

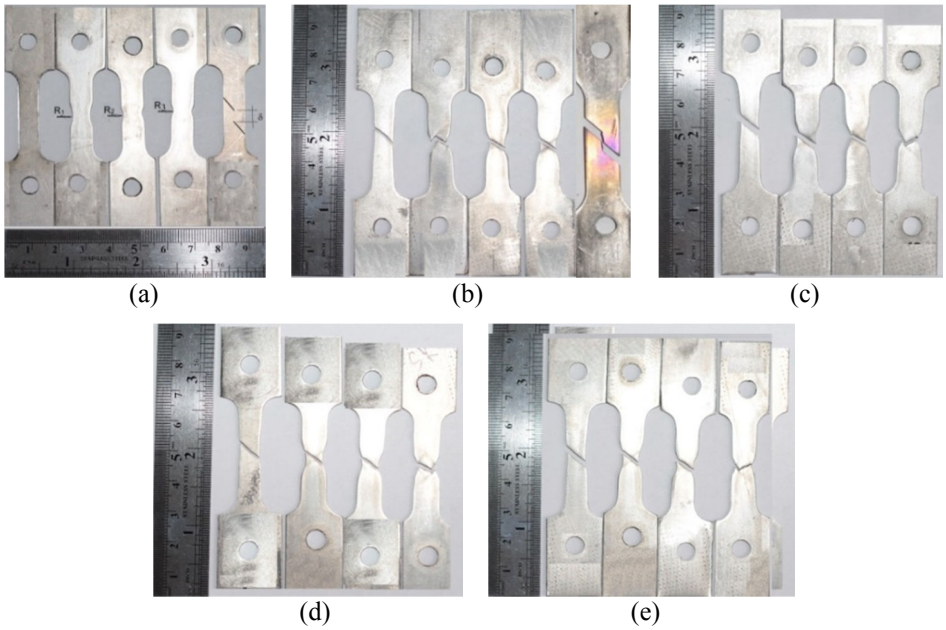

Fig. 1 (a) Geometry of the samples used for tensile and shear tests: l_0 =24±0.1 mm, A_0=9.3±0.05 mm^2, notch radius: R_1=10 mm, R_2 = 5 mm, R_3=2 mm, distance between cuts δ =4.5 mm; (b) Fractured samples after tension at the velocity: 20 m/s; (c) 12 m/s; (d) 2.4 m/s; (e) 0.4 m/s

The samples of ~1.18+0.01 mm thickness were cut using electroerosion method from a sheet of titanium alloy. The initial length l_0 of samples was equal to 24±0.1 mm, the cross-sectional area of the smooth flat samples was A_0=9.3±0.05 mm^2, notch flat specimens had notch radius of R_1=10 mm, R_2 = 5 mm, R_3=2 mm, respectively. The samples for shear test had distance between cuts δ ~4.5 mm.

QUASISTATIC AND DYNAMIC TESTS

The tests were carried within the range of strain rates (16−833 s^{-1}) at room temperature using an Instron test machine VHS 40/50-20 with a 50 kN loadcell. The tests were conducted at constant tensile velocity 20±0.01, 12±0.01, 2.4±0.002, 0.4±0.001 m/s. Tests were divided into three groups: (I) uniaxial tensile tests carried out on smooth specimens, characterized by positive values of both the stress triaxiality and Lode parameter. The second group is pure shear tests. The third group is uniaxial tensile tests carried out on flat notch specimens. Two values of notch radius, 2 mm, and 10 mm, were used in this study. The true stress and the true stress were determined using the analytical formulas:

$$\varepsilon_1^{true} = \ln(1+\Delta l / l_0)\,,\ \sigma_1^{true} = (F / A_0)(1+\Delta l / l_0)\,, \tag{3}$$

where ε_1^{true} is true strain, σ_1^{true} is true stress, F is tensile force, A_0 is mean initial minimum cross sectional area of sheet sample, Δl is the change in gauge length, l_0 is the initial gauge length.

COMPUTATIONAL MODEL

The computational model uses the theoretical basis of continuum damage mechanics (Kachanov, 1958; Rabotnov,1963; Zhang, 2010). Mechanical behavior of smooth and notched dog-bone shaped flat specimens under tension was described by a system of conservation equations (mass, momentum and energy), a kinematic equation, and a constitutive equation. Computer simulations of deformation and fracture processes were performed using licensed software ANSYS 14.5 and being a part of the software LS-DYNA. The calculations were carried out with solvers using a finite difference scheme of second-order accuracy. Grid model of a dog-bone shape flat sample is shown in Figure 2.

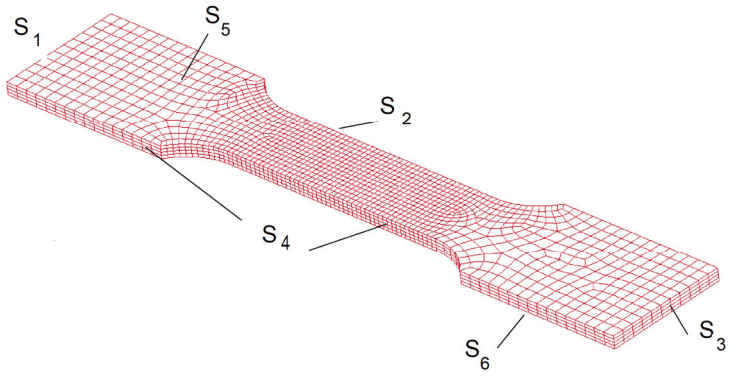

Fig. 2 - Grid model of a flat sample

The initial and boundary conditions were added to the system of equations. Initial condition corresponded to state of the material in uniform temperature field T_0:

$$\rho\big|_{t=0} = \rho_0\,,\ \varepsilon_{ij}\big|_{t=0} = 0,\ \sigma_{ij}\big|_{t=0} = 0,\ T\big|_{t=0} = T_0\,, \tag{4}$$

where t is a time, ρ is a mass density, σ_{ij} is components of stress tensor, T_0 is initial temperature

The boundary conditions (5) correspond to the conditions of loading of a 3D body. Dog-bone shape specimens were simulated under axial tension with a constant strain rate.

$$\begin{aligned} &u_x\,|_{S_1} = 0, \quad u_x\,|_{S_3} = 0, \\ &u_y\,|_{S_1} = 0, \quad u_y\,|_{S_3} = v_{y_0}, \\ &u_z\,|_{S_1} = 0, \quad u_z\,|_{S_3} = 0, \\ &\sigma_{ij}\,|_{S_2 \cup S_4 \cup S_5 \cup S_6} = 0, \end{aligned} \tag{5}$$

where $u_i\,|_{S_j}$ are the components of the mass velocity vector on the surface S_j, v_{y_0} is the tensile velocity, σ_{ij} is the components of the stress tensor.

Plastic flow was described within the theory of Prandtl-Reuss with the von Mises criterion. The flow stress of zirconium alloys under loading has been described using a modification of the Johnson-Cook model (6) (Johnson, 1985) and the Zerilli-Armstrong model for α-phase alloy (7) and β-phase alloy (8) (Zerilli, 1992; Gao, 2011; Abed, 2005):

$$\sigma_s(\varepsilon^p_{eq}, \dot{\varepsilon}_{eq}, T) = (a + k_h d_g^{-1/2} + b(\varepsilon^p_{eq})^n)(1 + c\ln(\dot{\varepsilon}_{eq}/\dot{\varepsilon}_0))(1 - \bar{T}^m)\,, \tag{6}$$

$$\sigma_s(\varepsilon^p_{eq}, \dot{\varepsilon}_{eq}, T) = C_0 + k_h d_g^{-1/2} + C_5(\varepsilon^p_{eq})^{n_1} \exp\left(C_4\, T \ln(\dot{\varepsilon}_{eq}/\dot{\varepsilon}_0)\right)\{1 - [-C_3 T \ln(\dot{\varepsilon}_{eq}/\dot{\varepsilon}_0)]^q\}^p\,, \tag{7}$$

$$\sigma_s(\varepsilon^p_{eq}, \dot{\varepsilon}_{eq}, T) = C_0 + k_h d_g^{-1/2} + C_1 \exp\left(-C_3\, T + C_4\, T \ln(\dot{\varepsilon}_{eq}/\dot{\varepsilon}_0)\right) + C_5(\varepsilon^p_{eq})^{n_1}, \tag{8}$$

where $\varepsilon^p_{eq} = [(2/3)\varepsilon^p_{ij}\varepsilon^p_{ij}]^{1/2}$, $\dot{\varepsilon}_{eq} = [(2/3)\dot{\varepsilon}_{ij}\dot{\varepsilon}_{ij}]^{1/2}$, $\dot{\varepsilon}_0 = 1.0\,s^{-1}$, a, b, c, n, m are the material parameters, T is the temperature, $\bar{T} = (T - T_r)/(T_m - T_r)$, T_r =295 K is room temperature, T_m is the melting temperature, k_h is the coefficient of the Hall-Petch relation, C_0, C_1, C_3, C_4, n_1, q, p are material constants, d_g is the grain size.. The melting temperature is assumed as ~1844 K.

The equations (6)-(8) take into account the influence of grain sizes on the flow stress at the quasi-static loading of titanium alloys (Skripnyak, 2017).

Johnson-Cook constitutive equation parameters of VT5-1 are shown in Table 2. Zerilli-Armstrong constitutive equation parameters for alpha-phase VT5-1 alloy are shown in Table 3. These parameter values can be used to describe the flow stress of VT5-1 alloy at a temperature $T \leq T_{pt}$. The temperature T_{pt} of α→β phase transition is assumed as ~ 1311±15 K for VT5-1 alloy.

Table 2 - Johnson-Cook equation parameters of VT 5-1 (Ti-5Al-22,5Sn) alloy

a, MPa	k_h, MPa μm$^{1/2}$	b, MPa	n	m	c
280	189.7	1050	0.25	0.65	0.022467

Table 3 - Zerilli-Armstrong equation parameters of VT 5-1 (Ti-5Al-22,5Sn) alloy

C_0, MPa	k_h, MPa μm$^{1/2}$	C_1, MPa	C_3, K^{-1}	C_4, K^{-1}	C_5, MPa	n_1	q	p
280	189,7	190	0.000877	0.0004	1050	0.25	2/3	2

Temperature in the material particles of deformed body was calculated by relation:

$$T = T_0 + (0.9/\rho C_p)\int_0^{\varepsilon^p_{eq}} \sigma_{eq}\, d\varepsilon^p_{eq}\ , \tag{9}$$

where T_0 is the initial temperature of specimen, ρ =4.41 g/cm^3 is mass density of alloy, C_p= 586 J/Kg K is the specific heat of the VT5-1 alloy.

Studies (Sharkeev, 2016) have shown a significant increase in the temperature in the zone of localization of plastic deformation and damage formed before the failure of the alpha-titanium alloy under tension.

The GTN model (Bai, 2008; Tvergaard, 2015) was used for analysis of stresses and strains in smooth and notched samples of sheet VT 5-1 under tension. The yield criterion has a form:

$$(\sigma_{eq}{}^2/\sigma_s{}^2) + 2q_1 f^* \cosh(-q_2\, p/2\sigma_s) - 1 - q_3 (f^*)^2 = 0\,, \tag{10}$$

where σ_s is the yield stress, p is the pressure, q_1, q_2 and q_3 are model parameters, and f is the void volume fraction, $\sigma_{eq} = [(3/2)S_{ij}S_{ij}]^{1/2}$, $S_{ij} = \sigma_{ij} - \sigma_{kk}/3.$

The rate of void growth is obtained by assuming mass conservation and depends on the volume change part of the plastic strain.

Consequently, there is no void growth in pure shear deformation. The void nucleation depends on the equivalent plastic strain ε_p, here a normal distribution A is used:

A strong coupling between deformation and damage is introduced by a plastic potential function which is dependent on the void volume fraction f* (Neilsen, 2010).

$$\begin{aligned} \dot{f} &= \dot{f}_{nucl} + \dot{f}_{growth}, \\ \dot{f}_{nucl} &= (f_N/s_N)\dot{\varepsilon}^p \exp\{-0.5[\varepsilon^p{}_{eq} - \varepsilon_N)/s_N]^2\}, \\ \dot{f}_{growth} &= (1-f)\dot{\varepsilon}^p_{kk}, \end{aligned} \tag{11}$$

where ε_N and s_N are the average nucleation strain and the standard deviation respectively. The amount of nucleating voids is controlled by the parameter f_N.

$$\begin{aligned} f^* &= f \ \text{if}\ f \le f_c; \\ f^* &= f_c + (\bar{f}_F - f_c)/(f_F - f_c)\ \text{if}\ f > f_c, \end{aligned} \tag{12}$$

where $\bar{f}_F = (q_1 + \sqrt{q_1{}^2 - q_3})/q_3$, q_1,q_2, and q_3 are constants of the model.

The final stage in ductile fracture comprises in the voids coalescence into the fracture zone. This causes softening of the material and accelerated growth of the void fraction f* until the

fracture void fraction f_F is reached. At this moment the material is fractured. The model of ductile fracture requires knowledge of 9 parameters: three model parameters (q_1, q_2 and q_3), the initial void fraction f_0, three void nucleation parameters (ε_N, s_N and f_N), two failure parameters (f_c and f_F). The model parameters for titanium alloy VT 5-1 were determined by numerical simulation of experiments on the tensile samples in the velocity range from 20 to 0.4 m/s. Numerical values of model parameters are given in Table 4.

Table 4 - Dimensionless parameters of the GTN model for the VT 5-1 (Ti-5Al-22,5Sn) sheets

Parameter	q_1	q_2	q_3	f_0	f_N	fc	f_F	ε_N	s_N
	1	0.7	1	0.003	0.1156	0.117	0.260	0.05	0.005

The model was used for simulation of titanium samples under tension at constant velocity from 20 m/s to 0.4 m/s.

RESULTS AND DISCUSSION

The tensile tests were performed on samples of VT 5-1 (Ti-5Al-22,5Sn) alpha titanium alloy characterized by different geometries, in order to vary both the stress triaxiality and Lode parameter. The tests were carried within the range of strain rates ($16-833\ s^{-1}$) at room temperature using an Instron test machine VHS 40/50-20 with a 50 kN loadcell. The tests were conducted at constant tensile velocity 20±0.01, 12±0.01, 2.4±0.002, 0.4±0.001 m/s. Tests were divided into three groups: (I) uniaxial tensile tests carried out on smooth specimens, characterized by positive values of both the stress triaxiality and Lode parameter. The second group is pure shear tests. The third group is uniaxial tensile tests carried out on flat notch specimens. Two values of notch radius, 2 mm, and 10 mm, were used in this study.

The true stress versus true strain at room temperature and strain rate 834 s^{-1} (at the velocity 20 m/s) are shown in Figure 1(a). Measured values of strain to fracture at strain rates 833±5, 418 ±2, 100±1, 16.7±1 s^{-1} of smooth and notch samples are shown in Figure 1(b).

Photos of fractured samples after tension are showed in Figure 1(b). The true flow stress versus true strain at room temperature and strain rate 834 s^{-1} (at the velocity 20 m/s) are shown in Figure 1(a). Measured values of strain to fracture at strain rates 833±5, 418 ±2, 100±1, 16.7±1 s^{-1} of smooth and notch samples are shown in Figure 1(b).

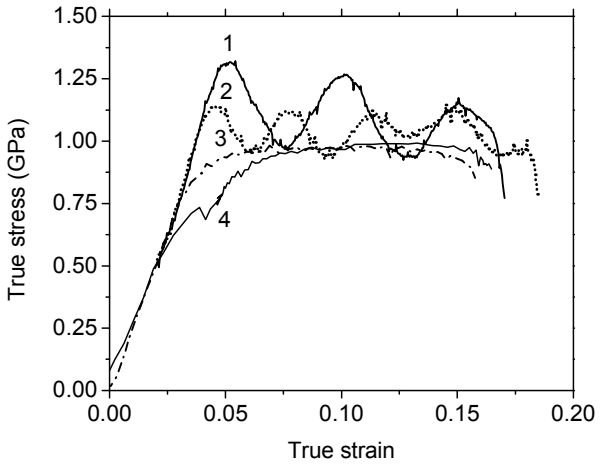

Fig. 3 - True flow stress versus true strain for smooth samples (η=0.33) at room temperature. Curves 1-4 correspond to velocities of tension: 20±0.01, 12±0.01, 2.4±0.002, 0.4±0.001 m/s, respectively.

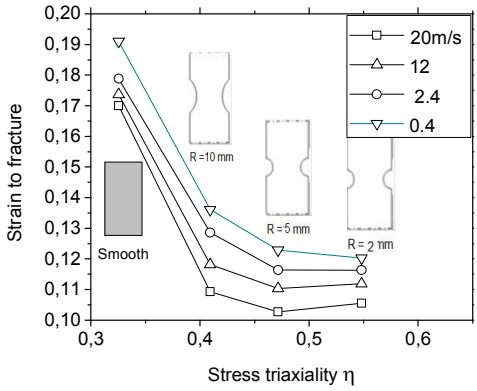

Fig. 4 - Strain to fracture of titanium VT 5-1 samples under axial tension at velocities 20, 12, 2.4, 0.4 m/s and at the initial stress triaxiality η: 0.3333, 0.4087, 0.4681, and 0.5491.

Calculated effective plastic strains, effective stresses, and tensile strength in the notched sample with R=10 mm are shown in Figures 3 and 4. Velocity of tension is 20 m/s. Figures 5 (a), (c), (e) corresponds to strain of 0.11. The simulations demonstrate the important role of strain localization phenomena in the fracture processes. The calculated plastic strain distributions in the necked zone around the center of the flat sheet sample are presented in Figure 3(a). Around the center, two shear bands are formed. Figures 5 (b), (d), (f) show the configuration of crack. Calculated crack have good agreement with experimental data (see Figure 1 (b)). Good agreement of the location, shape and length of the cracks with the received in this work experimental data was obtained also at tension velocities 12, 2.4 and 0.4 m/s.

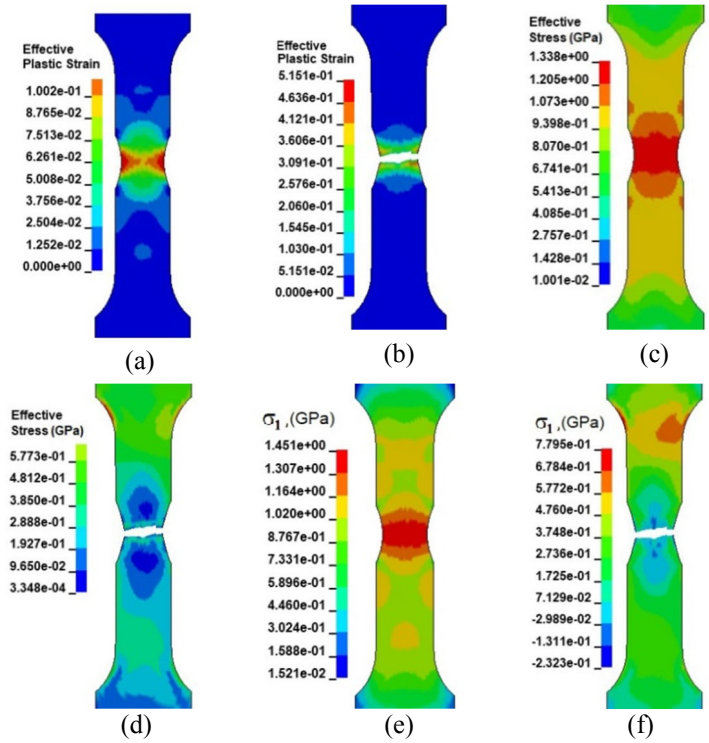

Fig. 5 - (a), (b) Calculated effective plastic strain, (c), (d) effective stress, and (e), (f) σ1 tensile stress under axial tension at the velocity ~20 m/s

The simulation results in Figure 6 demonstrate that changes in stress triaxiality in the necking zone have a significant influence on the plastic flow stress and evolution of damage in the alpha titanium alloys at high strain rates. Therefore, the true stress obtained from analytical relations (3) is underestimated relative to the values obtained by numerical simulation. The introduction of the stress triaxiality in the plastic flow model is important for prediction of damage evolution under deformation especially at high strain rates.

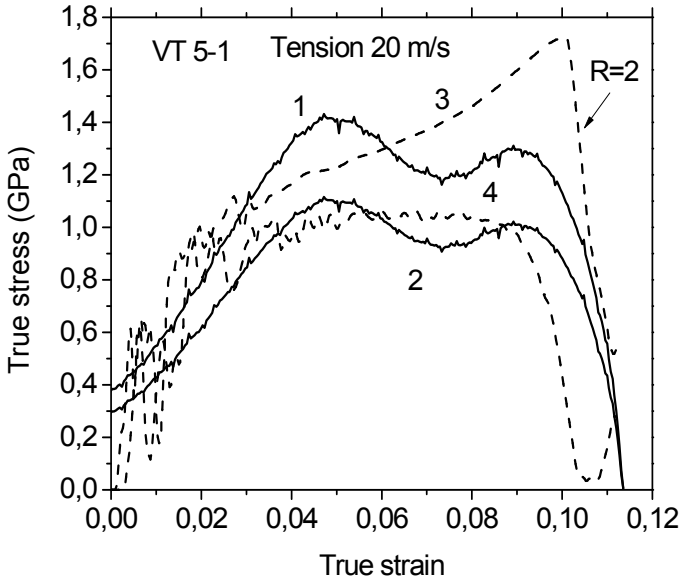

Fig. 6 - Analytical (curves (1), and (2)) and numerically calculated (curves (3), and (4)) true strain versus true stress in notch sample (R=2 mm) at the velocity of tension 20 m/s. Curves (1), and (3) correspond to notch zone. Curves (2) and (4) correspond to smooth zone of samples.

Damage kinetics in alpha titanium alloys is connected with macroscale plastic instability. This paper presents the experimental and theoretical results that demonstrate the importance of an adequate description of the processes of instability of deformation in titanium alloys. The study of instabilities of plastic deformation of HCP alloys including a test at elevated temperatures below temperature of $\alpha \rightarrow \beta$ phase transition is of interest for the development of promising engineering applications.

SUMMARY AND CONCLUSIONS

Tensile tests at strain rates from 0.01 to ~850 s^{-1} were carried out on smooth and notched sheet samples of VT5-1 alloys in order to simultaneously change stress triaxiality and Lode parameter. It was found that strain rate in the range from 10 to ~850 s^{-1} and stress triaxiality factor are noticeable influenced on the yield stress and the strain to fracture of alpha titanium alloy. Parameters of Johnson-Cook and Zeriillii-Armstrong constitutive equations and Gurson-Tvergaard-Needleman failure model of VT 5-1 alloy were estimated using the tensile test results. The constitutive equations and fracture model were calibrated by numerical simulation of the mechanical behavior of VT 5-1 alloy under tension in a wide range of strain rates. A good predictability of the strain to fracture of alpha titanium alloy was shown the as function of strain rate and temperature.

ACKNOWLEDGMENTS

This work was partially supported by the Russian Science Foundation (RSF), grant No. 16-1910264, the grant from the President of Russian Federation MK-2690.2017.8, and the grant from the Foundation of D. I. Mendeleev National research Tomsk State University within the program of increasing the competitiveness of TSU. The authors are grateful for the support of this research.

REFERENCES

[1] Abed F., Voyiadijs G.Z. A consistent modified Zerilli-Armstrong flow stress model for BCC and FCC metals for elevated temperatures//Acta Mechanica, 2005, 175(1), pp. 1-18.

[2] Bai Y., Wierzbicki T. A new model of metal plasticity and fracture with pressure and Lode dependence // International Journal of Plasticity, 2008, 24, pp. 1071-1096.

[3] Bobbili R., Madhu V. Effect of strain rate and stress triaxiality on tensile behavior of Titanium alloy Ti-10-2-3 at elevated temperatures // Materials Science & Engineering A, 2016, 667, pp. 33-41.

[4] Gao C.Y., Zhang L.C., Yan H.X. A new constitutive model for HCP metals // Materials Science & Engineering A, 2011, pp. 4445-4452.

[5] Johnson G.R., Cook W.H. Fracture characteristics of three metals subjected to various strains, strain rates, temperatures and pressures // Eng. Fract. Mech., 1985, 21, pp. 31-48.

[6] Kachanov L.M. Time of the rupture process under creep conditions // Izv. Akad Nauk SSSR. Otd Teckh Nauk, 1958, 8, pp. 26-31.

[7] Neilsen K.L., Tvergaard V. Ductile shear failure or plug failure of spot welds modelled by modified Gurson model.// Eng. Fract. Mech., 2010, 77, pp.1031-1047.

[8] Rabotnov Y.N. On the equations of state for creep //Prog Appl Mech., Prag Anniv 1963, pp. 307-315.

[9] Selini N., Elmeguenni M., Benguediab M. Effect of the Triaxiality in Plane Stress Conditions // Eng. Technol. & Appl. Sci. Res. 2013, 3, pp. 373-380.

[10] Sharkeev Y.P., Belyavskaya O.A., Vavilov V.P., Nesteruk D.A., Skripnyak V.A., Kozulin A.A., Kim V.M. Analyzing deformation and damage of VT1-0 titanium in different structural states by using infrared thermography //Journal of Nondestructive Evaluation, 2016, 35(3) pp. 42-46.

[11] Skripnyak V.A., Skripnyak E.G. Mechanical behavior of nanostructured and ultrafine-grained metal alloy under intensive dynamic loading // Nanotechnology and Nanomaterials, (ed.) A. Vakhrushev, Chapter 2, 2017. ISBN 978-953-51-3182-3.

[12] Skripnyak V.A., Skripnyak N.V., Skripnyak E.G., Skripnyak V.V. Influence of grain size distribution on the mechanical behaviour of light alloys in wide range of strain rates //AIP Conference Proceedings 1793, 110001, 2017, 4p.

[13] Tvergaard V. Behaviour of porous ductile solids at low stress triaxiality in different modes of deformation //International Journal of Solids and Structure, 2015, 60-61, pp. 28-34.

[14] Valoppi B., Bruschi S., Ghiotti A., Shivpuri R. Johnson-Cook based criterion incorporating stress triaxiality and deviatoric effect for predicting elevated temperature ductility of titanium alloy sheets// Int. J. of Mech. Sci., 2017, 123, pp. 94-10.

[15] Zerilli F.J., Armstrong R.W. The effect of dislocation drag on the stress-strain behaviour of F.C.C. metals // Acta Metall. Mater, 1992, 40, pp. 1803-1808.

[16] Zhang W., Cai Y. Continuum Damage Mechanics and Numerical Applications. Springer Science & Business Media, 2010 - Technology & Engineering, 1000 p. ISBN 978-3-642-04708-4 (eBook).